

SWAT 98/212
CERN-TH/98-398

The Proton-Spin Crisis: another ABJ anomaly?

G.M. Shore

*Department of Physics, University of Wales Swansea
Singleton Park, Swansea, SA2 8PP, U.K.*

and

*Theory Division, CERN
CH 1211 Geneva 23, Switzerland*

Contents:

1. Introduction
2. The First Moment Sum Rule for g_1^p
3. The Parton Model and the ‘Proton Spin’
4. The CPV Method and Topological Charge Screening
5. Experiment
6. Semi-Inclusive Polarised DIS

1. Introduction

For a decade, the ‘proton spin’ problem – the anomalous suppression observed in the flavour singlet component of the first moment of the polarised proton structure function $g_1^p(x; Q^2)$ – has puzzled and intrigued theorists and experimentalists alike. The consequent research effort has indeed been impressive: to date, the original EMC paper[1] alone has nearly one thousand citations.

In this lecture, we first give a brief review of the ‘proton spin’ problem from the standard viewpoint of the parton model. We explain why the 1988 observation by the EMC of a violation of the Ellis-Jaffe sum rule[2] for g_1^p was initially mis-interpreted in terms of quark spins and how the problem is resolved in the context of the full QCD parton model[3].

* *Lecture presented at the International School of Subnuclear Physics, ‘From the Planck Length to the Hubble Radius’, Erice, 1998.*

SWAT 98/212
CERN-TH/98-398
December 1998

We then describe an alternative, complementary approach to the description of deep inelastic scattering (DIS), the ‘CPV’ method[4-6], which allows the problem to be viewed in a new light. From this perspective, the Ellis-Jaffe sum rule is simply seen to be equivalent to the OZI approximation for the forward proton matrix element of the flavour singlet axial current. The ‘proton spin’ problem is therefore one of understanding the origin of the OZI violation observed in this channel[7]. As such, it is one more addition to the collection of ‘ $U_A(1)$ problems’ in QCD – phenomena whose interpretation depends on the presence of the ABJ axial anomaly[8] and the implicit relation with gluon topology (see e.g. ref.[9]). As we shall show, the observed suppression in the first moment of g_1^p is due to *topological charge screening* by the QCD vacuum itself, and a quantitative resolution in terms of an anomalous suppression of the slope of the gluon topological susceptibility is proposed.

An immediate consequence of this explanation is that the suppression in g_1^p is in fact a *target independent* phenomenon, which would in principle be true for polarised DIS on any hadronic target. Not only is the ‘proton spin’ problem nothing to do with spin – it is not even a special property of the proton! To test this idea, we have proposed[10,11] a set of semi-inclusive polarised DIS experiments, which could be performed at e.g. polarised HERA, and which would provide independent confirmation of the mechanism of topological charge screening by the QCD vacuum.

2. The First Moment Sum Rule for g_1^p

The structure function g_1^p is measured in polarised DIS experiments through the inclusive processes $\mu p \rightarrow \mu X$ (EMC, SMC) or $ep \rightarrow eX$ (SLAC, HERMES). See Fig. 1.

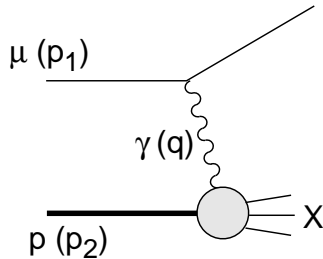


Fig.1 Inclusive polarised DIS scattering.

The polarisation asymmetry of the cross section is expressed as

$$x \frac{d\Delta\sigma}{dx dy} = \frac{Y_P}{2} \frac{16\pi^2 \alpha^2}{s} g_1^p(x, Q^2) + O\left(\frac{M^2 x^2}{Q^2}\right) \quad (2.1)$$

where the omitted terms include the second polarised structure function g_2^p . The notation is standard: $Q^2 = -q^2$ and $x = \frac{Q^2}{2p_2 \cdot q}$ are the Bjorken variables, $y = \frac{Q^2}{xs}$ and $Y_p = \frac{2-y}{y}$.

According to standard theory, g_1^p is determined by the proton matrix element of two electromagnetic currents carrying a large spacelike momentum. The sum rule for the first moment (w.r.t. Bjorken x) of g_1^p is derived using the twist 2, spin 1 terms in the OPE for

the currents:

$$J^\rho(q)J^\sigma(-q) \underset{Q^2 \rightarrow \infty}{\sim} 2\epsilon^{\rho\sigma\nu\mu} \frac{q_\nu}{Q^2} \left[C_1^{NS}(\alpha_s) \left(A_\mu^3 + \frac{1}{\sqrt{3}} A_\mu^8 \right) + \frac{2}{3} C_1^S(\alpha_s) A_\mu^0 \right] \quad (2.2)$$

where C_1^{NS} and C_1^S are the Wilson coefficients and A_μ^a ($a = 0, 3, 8$) are the renormalised $SU(3)$ flavour axial currents. The sum rule is therefore:

$$\Gamma_1^p(Q^2) \equiv \int_0^1 dx g_1^p(x, Q^2) = \frac{1}{12} C_1^{NS} \left(a^3 + \frac{1}{3} a^8 \right) + \frac{1}{9} C_1^S a^0(Q^2) \quad (2.3)$$

where the axial charges a^3 , a^8 and $a^0(Q^2)$ are defined as the form factors in the forward proton matrix elements of the axial current, i.e.

$$\langle p, s | A_\mu^3 | p, s \rangle = s_\mu \frac{1}{2} a^3 \quad \langle p, s | A_\mu^8 | p, s \rangle = s_\mu \frac{1}{2\sqrt{3}} a^8 \quad \langle p, s | A_\mu^0 | p, s \rangle = s_\mu a^0(Q^2) \quad (2.4)$$

Here, p_μ and $s_\mu = \bar{u}\gamma_\mu\gamma_5 u$ are the momentum and polarisation vector of the proton respectively.

It is important in what follows to be precise about the renormalisation group properties of the operators and matrix elements which occur. The flavour non-singlet axial currents are not renormalised, but because of the $U_A(1)$ anomaly the flavour singlet current A_μ^0 is not conserved and therefore can, and does, have a non-trivial renormalisation. Defining the bare operators by $A_{\mu B}^a = \sum \bar{q}\gamma_\mu\gamma_5 T^a q$ and $Q_B = \frac{\alpha_s}{8\pi} \epsilon^{\mu\nu\rho\sigma} \text{tr} G_{\mu\nu} G_{\rho\sigma}$, (where $T^{a \neq 0}$ are $SU(n_f)$ flavour generators, $T^0 = \mathbf{1}$, and d -symbols are defined by $\{T^a, T^b\} = d_{abc} T^c$), the renormalised operators A_μ , Q , are given by[12]

$$A_\mu^{a \neq 0} = A_{\mu B}^{a \neq 0} \quad A_\mu^0 = Z A_{\mu B}^0 \quad Q = Q_B - \frac{1}{2n_f} (1 - Z) \partial^\mu A_{\mu B}^0 \quad (2.5)$$

where Z is a divergent renormalisation constant, the associated anomalous dimension being denoted by γ . Q is the gluon topological charge density – for field configurations which tend to a pure gauge at infinity, it satisfies

$$\int d^4x Q = n \in \mathbf{Z} \quad (2.6)$$

where n is the topological winding number, or ‘instanton’ number.

The link between quark dynamics in the flavour singlet $U_A(1)$ channel and gluon topology is provided by the famous $U_A(1)$ axial (or ABJ) anomaly⁽¹⁾:

$$\partial^\mu A_\mu^0 - 2n_f Q \sim 0 \quad (2.7)$$

⁽¹⁾ In this lecture, we will quote results only in the chiral limit of QCD, i.e. with massless quarks. The inclusion of quark masses, which produces only a small change in our final predictions, is described in detail in ref.[13].

where the symbol \sim denotes weak operator equivalence. Notice that with the definitions (2.5), this condition is the same expressed in terms of either the bare or renormalised operators.

A more complete formulation of the anomaly is given by introducing the generating functional $W[S_\mu^a, \theta, S_5^a, S^a]$ of connected Green functions (correlation functions) of the axial currents and the pseudoscalar operators Q and ϕ_5^a , where $\phi_{5B}^a = \sum \bar{q}\gamma_5 T^a q$ (together with the corresponding scalar ϕ^a). Here, $S_\mu^a, \theta, S_5^a, S^a$ are the sources for $A_\mu^a, Q, \phi_5^a, \phi^a$ respectively. The (anomalous) Ward identities are then expressed as

$$\partial_\mu \frac{\delta W}{\delta S_\mu^a} - 2n_f \delta_{a0} \frac{\delta W}{\delta \theta} + d_{adc} S^d \frac{\delta W}{\delta S_5^c} - d_{adc} S_5^d \frac{\delta W}{\delta S^c} = 0 \quad (2.8)$$

where the final two terms account for the chiral variations of the operators ϕ_5^a, ϕ^a . (For a more extensive description of this formalism, see refs.[5,9].) Ward identities for 2-point Green functions (composite operator propagators) are then derived by taking functional derivatives w.r.t. the relevant sources. For example,

$$\partial_\mu W_{S_\mu^0 \theta} - 2n_f W_{\theta\theta} = 0 \quad (2.9)$$

where for simplicity we adopt a notation where functional derivatives are denoted by subscripts and integrals over spacetime are assumed as appropriate. Since there is no massless $U_A(1)$ Goldstone boson in the physical spectrum (resolution of the $U_A(1)$ problem), the first term vanishes at zero momentum, leaving⁽²⁾ ⁽³⁾

$$W_{\theta\theta}|_{k=0} = 0 \quad (2.10)$$

The renormalisation group equations (RGEs) implied by eq.(2.5) can also be conveniently written in a functional form. The fundamental RGE for the generating functional W is[5,9]

$$\mathcal{D}W = \gamma \left(S_\mu^0 - \frac{1}{2n_f} \partial_\mu \theta \right) W_{S_\mu^0} + \gamma_\phi \left(S_5^a W_{S_5^a} + S^a W_{S^a} \right) + \dots \quad (2.11)$$

where $\mathcal{D} = \left(\mu \frac{\partial}{\partial \mu} + \beta \frac{\partial}{\partial g} \right) \Big|_{V, \theta, S_5, S}$ and γ_ϕ is the anomalous dimension corresponding to the pseudoscalar (or scalar) composite field renormalisation. The notation $+\dots$ refers to the additional terms which are required to produce the contact terms in the RGEs for Green functions involving more than one composite operator. These vanish at zero momentum and need not be considered here.

The RGEs for 2-point Green functions follow immediately by functional differentiation of eq.(2.11). For example, differentiating twice w.r.t. θ , and using the Ward identity (2.9), we find

$$\mathcal{D}W_{\theta\theta} = 2\gamma W_{\theta\theta} + \dots \quad (2.12)$$

⁽²⁾ Here, and elsewhere throughout the text, I have included a discussion of points omitted during the lecture itself which were subsequently raised in the discussion sessions.

⁽³⁾ In fact, the same conclusion would hold even if there were a physical massless boson coupling derivatively to the $U_A(1)$ current since, in momentum space, the residue of the pole at $k^2 = 0$ in the first term in eq.(2.9) due to this boson would itself be $O(k^4)$.

We are focusing on results for $W_{\theta\theta}$ here because it is a key correlation function in QCD which will play a central role in our analysis of the ‘proton spin’ problem. It is called the *topological susceptibility*, and is usually denoted by χ . In conventional notation,

$$\chi(k^2) \equiv W_{\theta\theta}(k^2) = i \int d^4x e^{ikx} \langle 0|T Q(x) Q(0)|0 \rangle \quad (2.13)$$

Returning to the structure function sum rule (2.3), we can now deduce the RG behaviour of the axial charges. From either (2.5) or (2.11), we see immediately that

$$\frac{d}{dt} a^{3,8} = 0 \quad \frac{d}{dt} a^0(Q^2) = \gamma a^0(Q^2) \quad (2.14)$$

where $t = \ln Q^2/\Lambda^2$. The singlet axial charge is therefore scale dependent. This is crucial in understanding the ‘proton spin’ problem in QCD.

The flavour non-singlet axial charges a^3 and a^8 are known in terms of the F and D constants found from neutron and hyperon beta decay:

$$a^3 = F + D \quad a^8 = 3F - D \quad (2.15)$$

The interest of the sum rule therefore centres on the flavour singlet axial charge $a^0(Q^2)$. In the absence of an alternative experimental determination of $a^0(Q^2)$, the simplest ansatz is to assume that it obeys the OZI rule, i.e. $a^0(Q^2) = a^8$. In precise terms, the OZI limit of QCD is defined[14] as the truncation of full QCD in which non-planar and quark-loop diagrams are retained, but diagrams in which the external currents are attached to distinct quark loops, so that there are purely gluonic intermediate states, are omitted. (This last fact makes the connection with the familiar phenomenological form of the OZI, or Zweig, rule.) This is a more accurate approximation to full QCD than either the leading large $1/N_c$ limit, the quenched approximation (small n_f at fixed N_c) or the leading topological expansion ($N_c \rightarrow \infty$ at fixed n_f/N_c). In the OZI limit, the $U_A(1)$ anomaly is absent, there is no meson-gluon mixing, and there is an extra $U_A(1)$ Goldstone boson.

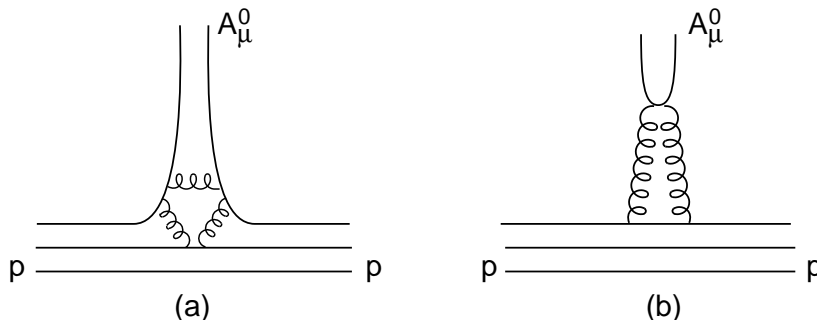


Fig.2 ‘Connected’ (a) and ‘disconnected’ (b) contributions to the matrix element $\langle p|A_\mu^0|p \rangle$. Diagrams of type (b) are suppressed in the OZI limit.

Applied to the axial charges, the OZI rule states that of the two valence quark diagrams shown in Fig. 2 describing the coupling of the axial current to the proton, the diagram in Fig. 2(b) is suppressed. Since this is the only way the s -quark component of either A_μ^0 or A_μ^8 can couple to the proton (uud), the OZI prediction $a^0 = a^8$ follows immediately.

Inserted into the sum rule (2.3), the OZI approximation $a^0(Q^2) = a^8$ gives a theoretical prediction for Γ_1^p which is known as the Ellis-Jaffe sum rule. This is now known to be violated, with $a^0(Q^2)$ strongly suppressed (by a factor of around 0.5) relative to a^8 . This experimental result, which was first discovered by the EMC collaboration and confirmed and improved in the subsequent decade of experimental work, is what has come to be known as the ‘proton spin’ problem (or even crisis!).

In fact, it is not at all surprising that the OZI rule should fail in this case[7,4,5]. The first clue is the anomaly-induced scale dependence of $a^0(Q^2)$. If the OZI rule were to hold, at what scale should it be applied? Moreover, it is known that the pseudovector and pseudoscalar channels are linked through the Goldberger-Treiman relations. Since large anomaly-induced OZI violations are known to be present in the pseudoscalar channel ($U_A(1)$ problem, η' mass, etc.) it is natural to find them also for $a^0(Q^2)$ in the pseudovector channel. It is also immediately clear from its scale-dependence that $a^0(Q^2)$ cannot really measure spin.

While this immediately resolves the ‘proton spin’ *problem*, clearly we want to understand the origin of the suppression in $a^0(Q^2)$ much more deeply. In the next two sections, we describe two complementary approaches to this question – the conventional QCD parton model and the CPV method developed in refs.[4-6].

3. The Parton Model and the ‘Proton Spin’

In the simplest form of the parton model, the proton structure for large Q^2 DIS is described by parton distributions corresponding to free valence quarks only. The polarised structure function is given by

$$g_1^p(x) = \frac{1}{2} \sum_{i=1}^{n_f} e_i^2 \Delta q_i(x) \quad (3.1)$$

where $\Delta q_i(x) = q_i^+(x) + \bar{q}_i^+(x) - q_i^-(x) - \bar{q}_i^-(x)$ is defined as the difference of the distributions of quarks (and antiquarks) with helicities parallel and antiparallel to the nucleon spin. It is convenient to work with the flavour non-singlet and singlet combinations:

$$\Delta q^{NS}(x) = \sum_{i=1}^{n_f} \left(\frac{e_i^2}{\langle e^2 \rangle} - 1 \right) \Delta q_i(x) \quad \Delta q^S(x) = \sum_{i=1}^{n_f} \Delta q_i(x) \quad (3.2)$$

In this model, the first moment of the singlet quark distribution $\Delta q^S = \int_0^1 dx \Delta q^S(x)$ can be identified as the sum of the helicities of the quarks. Interpreting the structure function data *in this model* then leads to the conclusion that the quarks carry only a small fraction of the spin of the proton – the ‘proton spin’ problem. There is indeed a real contradiction between the experimental data and the *free valence quark* parton model.

However, this simple model leaves out many important features of QCD, the most important being gluons, RG scale dependence and the chiral $U_A(1)$ anomaly. When these

effects are included, in the QCD parton model, the naive identification of Δq^S with spin no longer holds and the experimental results for g_1^p are readily accommodated.⁽⁴⁾

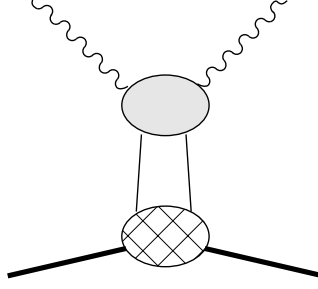


Fig.3 QCD parton model interpretation of DIS. The single lines are partons, which may be quarks or gluons.

The QCD parton model picture of DIS is shown in Fig. 3. The polarised structure function is written in terms of both quark and gluon distributions[3] as follows:

$$g_1^p(x, Q^2) = \frac{1}{9} \int_x^1 \frac{dy}{y} \left[C^{NS} \left(\frac{x}{y} \right) \Delta q^{NS}(y, t) + C^S \left(\frac{x}{y} \right) \Delta q^S(y, t) + C^g \left(\frac{x}{y} \right) \Delta g(y, t) \right] \quad (3.3)$$

where C^S , C^g and C^{NS} are perturbatively calculable functions related to the Wilson coefficients in sect. 2 and the quark and gluon distributions have *a priori* a $t = \ln Q^2/\Lambda^2$ dependence.

The RG evolution (DGLAP) equations for these polarised distributions are:

$$\frac{d}{dt} \Delta q^{NS}(x, t) = \frac{\alpha_s}{2\pi} \int_x^1 \frac{dy}{y} P_{qq}^{NS} \left(\frac{x}{y} \right) \Delta q^{NS}(y, t) \quad (3.4)$$

and,

$$\frac{d}{dt} \begin{pmatrix} \Delta q^S(x, t) \\ \Delta g(x, t) \end{pmatrix} = \frac{\alpha_s}{2\pi} \int_x^1 \frac{dy}{y} \begin{pmatrix} P_{qq}^S \left(\frac{x}{y} \right) & P_{qg} \left(\frac{x}{y} \right) \\ P_{gq} \left(\frac{x}{y} \right) & P_{gg} \left(\frac{x}{y} \right) \end{pmatrix} \begin{pmatrix} \Delta q^S(y, t) \\ \Delta g(y, t) \end{pmatrix} \quad (3.5)$$

⁽⁴⁾ Of course there is a separate angular momentum sum rule for the proton. The details are given in e.g. ref.[15]. The proton spin is given by the matrix element of the angular momentum operator \underline{J} :

$$J_i = \frac{1}{2} \epsilon_{ijk} \int d^3 \underline{x} M^{0jk}, \quad M^{\lambda\mu\nu} = x^\mu T^{\nu\lambda} - x^\nu T^{\mu\lambda}$$

where $T_{\mu\nu}$ is the energy-momentum tensor. This admits (up to equation of motion terms) a gauge-invariant decomposition into three terms which look like quark spin, quark orbital and total gluon angular momenta:

$$\underline{J} = \int d^3 \underline{x} \left[\sum q^\dagger \underline{\gamma} \gamma_5 q + \sum q^\dagger (\underline{x} \times i \underline{D}) q + \underline{x} \times (\underline{E} \times \underline{B}) \right]$$

We recognise here the operator $A_{\mu B}^0 = \sum \bar{q} \gamma_\mu \gamma_5 q$ which, *for free fields*, can be identified as the quark helicity operator. However, the composite operators in this expression must be renormalised and their scale dependence identified, and the above identifications then become more problematic. While it is interesting to pursue both the theory and experimental consequences of this sum rule[15], it is obvious that the axial charge $a^0(Q^2)$, given by the matrix element of the renormalised current A_μ^0 , is *not* measuring the spin of the proton.

showing the mixing between the singlet quark and the gluon distributions. The splitting functions P are also calculable in perturbative QCD, their moments being related to the anomalous dimensions of the series of increasing spin operators appearing in the OPE (2.2).

In this language, the first moment sum rule for g_1^p reads:

$$\Gamma_1^p(Q^2) = \frac{1}{9} \left[C_1^{NS} \Delta q^{NS} + C_1^S \Delta q^S + C_1^g \Delta g \right] \quad (3.6)$$

where Δq^{NS} , Δq^S and Δg are the first moments of the above distributions. Comparing with eq.(2.3), we see that the axial charge $a^0(Q^2)$ is identified with a linear combination of the first moments of the singlet quark and gluon distributions. It is often, though not always, the case that the moments of parton distributions can be identified in one-to-one correspondence with the matrix elements of local operators. The polarised first moments are special in that two parton distributions correspond to the same local operator.

The RG equations for the first moments of the parton distributions follow immediately from eqs.(3.4,3.5) and depend on the matrix of anomalous dimensions for the lowest spin, twist 2 operators. This introduces a renormalisation scheme ambiguity. The issue of scheme dependence has been studied thoroughly by Ball, Forte and Ridolfi[16] and an excellent summary can be found in ref.[17]. It is shown there that it is possible to choose a scheme known as the Adler-Bardeen or AB scheme (strictly, a class of schemes[16]) for which the parton distributions satisfy the following RG equations:

$$\begin{aligned} \frac{d}{dt} \Delta q^{NS} &= 0 & \frac{d}{dt} \Delta q^S &= 0 \\ \frac{d}{dt} \frac{\alpha_s}{2\pi} \Delta g(t) &= \gamma \left(\frac{\alpha_s}{2\pi} \Delta g(t) - \frac{1}{n_f} \Delta q^S \right) \end{aligned} \quad (3.7)$$

with the implication $C_1^g = -n_f \frac{\alpha_s}{2\pi} C_1^S$. It is then possible to make the following identifications with the axial charges:

$$\begin{aligned} a^3 &= \Delta u - \Delta d \\ a^8 &= \Delta u + \Delta d - 2\Delta s \\ a^0(Q^2) &= \Delta q^S - n_f \frac{\alpha_s}{2\pi} \Delta g(Q^2) \end{aligned} \quad (3.8)$$

where $\Delta u = \int_0^1 dx (\Delta u(x, t) + \Delta \bar{u}(x, t))$ etc. Notice that in the AB scheme, the singlet quark distribution $\Delta q^S = \Delta u + \Delta d + \Delta s$ (which is often written as $\Delta \Sigma$) is scale independent. All the scale dependence of the axial charge $a^0(Q^2)$ is assigned to the gluon distribution $\Delta g(Q^2)$. We emphasise that eq.(3.7) is true only in the AB renormalisation scheme and that it is only in this scheme that the identifications (3.8) hold.

This was the identification originally introduced for the first moments by Altarelli and Ross[3], and resolves the ‘proton spin’ problem in the context of the QCD parton model. In this picture, the Ellis-Jaffe sum rule follows from the assumption that in the proton both Δs and $\Delta g(Q^2)$ are zero. This is the natural assumption in the context of the

free valence quark model. It is equivalent to the naive OZI approximation $a^0(Q^2) = a^8$ described above. However, in the full QCD parton model, there is no reason why $\Delta g(Q^2)$, or even Δs , need be zero in the proton. Moreover, given the RG scale dependence of $a^0(Q^2)$, this assumption is *in contradiction with* QCD where the anomaly requires $a^0(Q^2)$ to scale with the anomalous dimension γ .

Since neither $\Delta\Sigma$ nor $\Delta g(Q^2)$ are currently measurable in other processes, the parton model is unable to make a quantitative prediction for the first moment Γ_1^p . While the model can accommodate the observed suppression, it cannot yet predict it.

An interesting conjecture, proposed in the original paper of Altarelli and Ross[3], is that the observed suppression in $a^0(Q^2)$ is due overwhelmingly to the gluon distribution $\Delta g(Q^2)$. If so, the strange quark distribution $\Delta s \simeq 0$ in the proton and so $\Delta\Sigma \simeq a^8$. Although by no means a necessary consequence of QCD, this is entirely plausible because it is the anomaly (which is due to the gluons and is responsible for OZI violations) which is responsible for the scale dependence in $a^0(Q^2)$ and $\Delta g(Q^2)$ whereas (in the AB scheme) $\Delta\Sigma$ is scale invariant. The essence of this conjecture will reappear in the next section where we describe the CPV method.

To test this conjecture, we need to find a way to measure $\Delta g(Q^2)$ itself, rather than the combination $a^0(Q^2)$. One possibility[16,18] is to exploit the different scaling behaviours of $\Delta q^S(x)$ and $\Delta g(x, Q^2)$ to distinguish their contributions in measurements of $g_1^p(x, Q^2)$ at different values of Q^2 . A second is to extract $\Delta g(x, Q^2)$ from processes such as open charm production, $\gamma^* g \rightarrow c\bar{c}$, which will be studied in various forthcoming experiments at COMPASS, RHIC, etc.

4. The CPV Method and Topological Charge Screening

In this section, we shall discuss a less conventional approach to DIS based on a decomposition of matrix elements into products of composite operator propagators and their associated 1PI vertex functionals. This formalism has been developed in a series of papers[4-6,13] on the ‘proton spin’ problem. The starting point, as indicated above, is the use of the OPE in the proton matrix element of two currents. This gives the standard form for a generic structure function moment:

$$\int_0^1 dx x^{n-1} F(x; Q^2) = \sum_i C_i^n(Q^2) \langle p | \mathcal{O}_i^n(0) | p \rangle \quad (4.1)$$

where \mathcal{O}_i^n are the set of lowest twist, spin n operators in the OPE and $C_i^n(Q^2)$ the corresponding Wilson coefficients. In the CPV approach, we now factorise the matrix element into the product of composite operator propagators and vertex functions, as illustrated in Fig. 4.

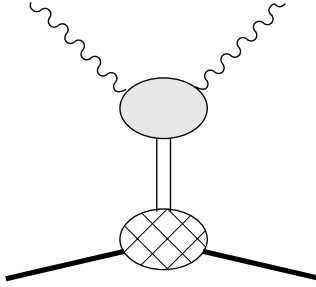


Fig.4 CPV description of DIS. The double line denotes the composite operator propagator and the lower blob the 1PI vertex.

To do this, we first select a set of composite operators $\tilde{\mathcal{O}}_i$ appropriate to the physical situation and define vertices $\Gamma_{\tilde{\mathcal{O}}_i pp}$ as 1PI with respect to this set. Formally, this is achieved by introducing sources for these operators in the QCD generating functional W , then performing a (partial) Legendre transform[5] to obtain a generating functional $\Gamma[\tilde{\mathcal{O}}_i]$. The 1PI vertices are the functional derivatives of $\Gamma[\tilde{\mathcal{O}}_i]$. The generic structure function sum rule (4.1) then takes the form

$$\begin{aligned} \int_0^1 dx x^{n-1} F(x, Q^2) &= \sum_i \sum_j C_j^{(n)}(Q^2) \langle 0|T \mathcal{O}_j^{(n)} \tilde{\mathcal{O}}_i|0\rangle \Gamma_{\tilde{\mathcal{O}}_i pp} \\ &= \sum_i \sum_j C_j P_{ji} V_i \end{aligned} \quad (4.2)$$

in a symbolic notation.

This decomposition splits the structure function into three pieces – first, the Wilson coefficients $C_j^{(n)}(Q^2)$ which control the Q^2 dependence and can be calculated in perturbative QCD; second, non-perturbative but *target-independent* QCD correlation functions $\langle 0|T \mathcal{O}_j^{(n)} \tilde{\mathcal{O}}_i|0\rangle$; and third, non-perturbative, target-dependent vertex functions $\Gamma_{\tilde{\mathcal{O}}_i pp}$ describing the coupling of the target proton to the composite operators of interest. The vertex functions cannot be calculated directly from first principles. They encode the information on the nature of the proton state and play an analogous role to the parton distributions in the more conventional parton picture.

It is important to recognise that this decomposition of the matrix elements into products of propagators and proper vertices is *exact*, independent of the choice of the set of operators $\tilde{\mathcal{O}}_i$. In particular, it is not necessary for $\tilde{\mathcal{O}}_i$ to be in any sense a complete set. All that happens if a different choice is made is that the vertices $\Gamma_{\tilde{\mathcal{O}}_i pp}$ themselves change, becoming 1PI with respect to a different set of composite fields. Of course, while any set of $\tilde{\mathcal{O}}_i$ may be chosen, some will be more convenient than others. Clearly, the set of operators should be as small as possible while still capturing the essential physics (i.e. they should encompass the relevant degrees of freedom) and indeed a good choice can result in vertices $\Gamma_{\tilde{\mathcal{O}}_i pp}$ which are both RG invariant and closely related to low energy physical couplings, such as $g_{\pi NN}$. In this case, eq.(4.2) provides a rigorous relation between high Q^2 DIS and low-energy meson-nucleon scattering.

For the first moment sum rule for g_1^p , it is most convenient to use the $U_A(1)$ anomaly equation immediately to re-express $a^0(Q^2)$ in terms of the forward matrix element of the

topological charge Q , i.e.

$$a^0(Q^2) = \frac{1}{2M} 2n_f \langle p|Q|p \rangle \quad (4.3)$$

where M is the nucleon mass.

Our set of operators \tilde{O}_i is then chosen to be the renormalised flavour singlet pseudoscalars Q and Φ_5 , where Φ_5 is simply the operator ϕ_5^0 of section 2 with a special, and crucial, normalisation. The normalisation factor is chosen such that in the OZI limit of QCD, where the anomaly is absent, Φ_5 would have the correct normalisation to couple with unit decay constant to the $U_A(1)$ Goldstone boson which would exist in this limit. This also ensures that the vertex is RG scale independent. (The proof may be found in refs.[5,13].) The vertices are defined from the generating functional $\Gamma[S_\mu^a, Q, \phi_5^a, \phi^a]$ where

$$\Gamma[S_\mu^a, Q, \phi_5^a, \phi^a] = W[S_\mu^a, \theta, S_5^a, S^a] - \int dx \left(\theta Q + S_5^a \phi_5^a + S^a \phi^a \right) \quad (4.4)$$

We then have

$$\Gamma_1^p{}_{singlet} = \frac{1}{9} \frac{1}{2M} 2n_f C_1^S(\alpha_s) \left[\langle 0|T Q Q|0 \rangle \hat{\Gamma}_{Qpp} + \langle 0|T Q \Phi_5|0 \rangle \hat{\Gamma}_{\Phi_5pp} \right] \quad (4.5)$$

where the propagators are at zero momentum and the vertices are 1PI w.r.t. Q and Φ_5 only. For simplicity, we have also introduced the notation $i\bar{u}\Gamma_{Qpp}u = \hat{\Gamma}_{Qpp}\bar{u}\gamma_5 u$, etc. This is illustrated in Fig. 5.

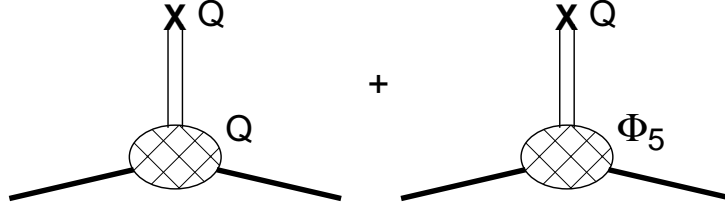


Fig.5 CPV decomposition of the matrix element $\langle p|Q|p \rangle$. The propagator in the first diagram is $\chi(0)$; in the second it is $\sqrt{\chi'(0)}$.

The composite operator propagator in the first term is simply the (zero-momentum) QCD topological susceptibility $\chi(0)$ which, as we have seen in section 2, vanishes for QCD with massless quarks. Furthermore, with the normalisation specified above for Φ_5 , the propagator $\langle 0|T Q \Phi_5|0 \rangle$ at zero momentum is simply the square root of the slope of the topological susceptibility.

To see this, notice that by virtue of their definition in terms of the generating functional (4.4), the matrix of 2-point vertices in the pseudoscalar sector is simply the inverse of the corresponding matrix of pseudoscalar propagators, i.e.

$$\begin{pmatrix} \Gamma_{QQ} & \Gamma_{Q\phi_5^0} \\ \Gamma_{\phi_5^0 Q} & \Gamma_{\phi_5^0 \phi_5^0} \end{pmatrix} = - \begin{pmatrix} W_{\theta\theta} & W_{\theta S_5^0} \\ W_{S_5^0 \theta} & W_{S_5^0 S_5^0} \end{pmatrix}^{-1} \quad (4.6)$$

This implies

$$\Gamma_{\phi_5^0 \phi_5^0} = -W_{\theta\theta} (\det W_{SS})^{-1} \quad (4.7)$$

letting \mathcal{S} represent the set $\{\theta, S_5^0\}$. Differentiating w.r.t. k^2 and taking the limit $k^2 = 0$, exploiting the fact that $W_{\theta\theta}(0)$ vanishes, we find

$$\frac{d}{dk^2}\Gamma_{\phi_5^0\phi_5^0}|_{k=0} = \chi'(0)W_{\theta S_5^0}^{-2}(0) \quad (4.8)$$

Finally, normalising the field Φ_5 proportional to ϕ_5^0 such that $\frac{d}{dk^2}\Gamma_{\Phi_5\Phi_5}|_{k=0} = 1$ (see refs.[5,13] for further discussion), we find the required relation

$$\langle 0|T Q \Phi_5|0\rangle|_{k=0} = \sqrt{\chi'(0)} \quad (4.9)$$

We therefore find:

$$\Gamma_{1 \text{ singlet}}^p = \frac{1}{9} \frac{1}{2M} 2n_f C_1^S(\alpha_s) \sqrt{\chi'(0)} \hat{\Gamma}_{\Phi_5 pp} \quad (4.10)$$

The slope of the topological susceptibility $\chi'(0)$ is not RG invariant but, as shown in eq.(2.12), scales with the anomalous dimension 2γ , i.e.

$$\frac{d}{dt}\sqrt{\chi'(0)} = \gamma\sqrt{\chi'(0)} \quad (4.11)$$

On the other hand, the proper vertex has been chosen specifically so as to be RG invariant[5,13]. The renormalisation group properties of this decomposition are crucial to our proposed resolution of the ‘proton spin’ problem.

Our proposal[4,5] is that we should expect the source of OZI violations to lie in the RG non-invariant, and therefore anomaly-sensitive, terms, i.e. in $\chi'(0)$ rather than in the RG invariant vertex. This is the key assumption that allows us to make a quantitative prediction for Γ_1^p on the basis of a calculation of the topological susceptibility alone. The RG invariance of the vertices is a necessary condition for this assumption to be reasonable. Further phenomenological evidence from $U_A(1)$ current algebra supporting this conjecture is discussed in refs.[5,19]. Notice that we are using RG non-invariance, i.e. dependence on the anomalous dimension γ , merely as an indicator of which quantities are sensitive to the anomaly and therefore likely to show OZI violations. Since the anomalous suppression in Γ_1^p is thus assigned to the composite operator propagator rather than the proper vertex, the suppression is a *target independent* property of QCD related to the anomaly, not a special property of the proton structure.

In this picture, therefore, the basic dynamical mechanism responsible for the suppression of the ‘proton spin’ can be identified as *topological charge screening* by the QCD vacuum. That is, when a matrix element of the topological charge is measured, the QCD vacuum screens the topological charge through the zero or anomalously small values of the susceptibility $\chi(0)$ and its slope $\chi'(0)$ respectively (see Fig. 4). The mechanism is analogous to the screening of electric charge in QED. There, because of the gauge Ward identity, the screening is given entirely by the (‘target independent’) dressing of the photon propagator by vacuum polarisation diagrams, leading to the relation $e_R = e_B\sqrt{Z_3}$ (with $Z_3 < 1$) between the renormalised and bare charges, in direct analogy to eq.(4.12) below with the topological susceptibility playing the role of the photon propagator.

To convert this into a quantitative prediction we use the OZI approximation⁽⁵⁾ for the vertex $\hat{\Gamma}_{\Phi_5 pp}$. In terms of a similarly normalised octet field Φ_5^8 , this is $\hat{\Gamma}_{\Phi_5 pp} = \sqrt{2}\hat{\Gamma}_{\Phi_5^8 pp}$. The normalisation is crucial in allowing the use of the OZI relation here. The corresponding OZI prediction for $\sqrt{\chi'(0)}$ would be $f_\pi/\sqrt{6}$. These OZI values are determined by comparing the result (4.10) (at least that part relating to the proton matrix element) with the conventional Goldberger-Treiman relation for the flavour octet axial charge in the chiral limit (see refs.[5,13]). This gives our key formula⁽⁶⁾

$$\frac{a^0(Q^2)}{a^8} = \frac{\sqrt{6}}{f_\pi} \sqrt{\chi'(0)}|_{Q^2} \quad (4.12)$$

for the flavour singlet axial charge. Incorporating this into the formula for the first moment of the polarised structure function, we find

$$\Gamma_1^p \text{ singlet} = \frac{1}{9} C_1^S(\alpha_s) a^8 \frac{\sqrt{6}}{f_\pi} \sqrt{\chi'(0)} \quad (4.13)$$

The final step involves an explicit calculation of $\chi'(0)$. This was done in ref.[6] using the QCD spectral sum rule (QSSR) method. We find[6,13]

$$\sqrt{\chi'(0)} = (26.4 \pm 4.1) \text{ MeV} \quad (4.14)$$

Substituting this in eq.(4.13), and also using the QSSR prediction for f_π in order to minimise systematic errors, we arrive at our prediction for the first moment of the polarised structure function in the chiral limit:

$$\begin{aligned} a^0(Q^2 = 10\text{GeV}^2) &= 0.33 \pm 0.05 \\ \Gamma_1^p(Q^2 = 10\text{GeV}^2) &= 0.144 \pm 0.009 \end{aligned} \quad (4.15)$$

⁽⁵⁾ Without this approximation, our result (4.12) reads:

$$\frac{a^0(Q^2)}{a^8} = \left(\frac{\sqrt{6}}{f_\pi} \sqrt{\chi'(0)}|_{Q^2} \right) \left(\frac{\hat{\Gamma}_{\Phi_5 pp}}{\sqrt{2}\hat{\Gamma}_{\Phi_5^8 pp}} \right) \equiv s_P s_V$$

A (target-independent) propagator suppression factor $s_P < 1$ is a signal of topological charge screening; a (target-dependent) vertex suppression factor $s_V < 1$ would be a sign that the proton coupling to the flavour singlet Goldstone boson η_{OZI}^0 in the OZI limit of QCD is small, equivalent in parton terms to a significant (negatively polarised) strange quark content in the proton. Of course both effects may be present. However, our conjecture is that the ‘proton spin’ problem is best explained by $s_P < 1$, $s_V \simeq 1$.

⁽⁶⁾ It is interesting to compare eq.(4.12) with the well-known Witten-Veneziano formula[20,21] which, at leading order in the $1/N_c$ expansion, relates the mass of the η' (in massless QCD) to χ^{YM} , the topological susceptibility of pure gluodynamics:

$$m_{\eta'} \simeq \frac{\sqrt{6}}{f_\pi} \sqrt{\chi^{YM}(0)}$$

This can be immediately compared with the Ellis-Jaffe sum rule prediction

$$a^0|_{\text{EJ}} = 0.58 \pm 0.03 \quad (4.16)$$

We therefore find a suppression of $a^0(Q^2)$ relative to the OZI expectation by a factor of around 0.55.

A complete description of our calculation of the slope of the topological susceptibility can be found in refs.[6,13]. The QSSR analysis of $\chi'(0)$ in the chiral limit of QCD is essentially straightforward and shows a clear range of stability with respect to the Laplace sum rule parameter τ , indicating that the prediction is reliable. The stabilisation scale, $\tau^{-1} \sim 2.5 - 5 \text{ GeV}^2$, is sufficiently big for higher dimensional condensates to be suppressed, and the calculation displays the hierarchy of gluonium to light meson hadronic scales anticipated by ref.[22].⁽⁷⁾

Lattice gauge theory methods may also be used to calculate the topological susceptibility. However, $\chi'(0)$ is a particularly difficult correlation function to calculate on the lattice, requiring algorithms that implement topologically non-trivial configurations in a sufficiently fast and efficient way. Very preliminary results from the Pisa group[26] of calculations in full QCD with dynamical quarks indicate a value of the order $\sqrt{\chi'(0)} \sim (19 \pm 4) \text{ MeV}$. Given the preliminary nature of the lattice simulations, the rough agreement with the QSSR result is encouraging. Qualitative explanations of topological charge screening and the anomalously small value of $\chi'(0)$ in QCD may also be given using models of the instanton vacuum, e.g. the instanton liquid model of ref.[27].

Finally, to complete this discussion, it is useful to recognise the complementary nature of the QCD parton model and the CPV method presented here. Both involve at present incalculable non-perturbative functions describing the proton state – the quark and gluon distributions in the parton picture and the 1PI vertices in the CPV method. Both exhibit a degree of universality – the same parton distributions may be used in different QCD processes such as DIS or hadron-hadron collisions, while the vertices (when they can be identified with low-energy couplings) also provide a link between high Q^2 DIS and soft meson-nucleon interactions.

The principal attribute of the parton model is that it allows a detailed description of the structure of the proton in terms of its quark and gluon constituents. On the other hand,

⁽⁷⁾ Nevertheless, our application of QSSR to the $U_A(1)$ sector of QCD has been criticised repeatedly by Ioffe (see e.g. refs.[23,24]) on two grounds: (i) that there are important neglected contributions from ‘instantons’, i.e. higher dimensional condensates, and (ii) that when the strange quark mass is included, QSSR results for current-current correlators show quite unrealistic $SU(3)$ breaking. Neither criticism is valid, and both are refuted in detail in our recent paper[13]. We have commented in the text how the size of the stabilisation scale is sufficient to suppress higher dimensional condensates. Ioffe’s second criticism is based on a calculation[25] where radiative corrections are not properly implemented and a number of other errors are made. The correct results are given in ref.[13], where we extend our previous analysis of the ‘proton spin’ problem systematically beyond the chiral limit using a new set of generalised Goldberger-Treiman relations.

one of the main advantages of the CPV method is that some non-perturbative information which is generic to QCD, i.e. independent of the target, is factored off into the composite operator propagator. This allows us to distinguish between non-perturbative mechanisms which are generic to all QCD processes and those which are specific to a particular target. As explained above, our contention is that the anomalous suppression in the first moment of g_1^p is of the first, target-independent, type. This conjecture could in principle be tested by DIS with non-nucleon targets, which may effectively be realised in semi-inclusive polarised DIS. This will be discussed in section 6.

Both the parton and CPV methods allow a natural conjecture in which the origin of this suppression is attributed to ‘glue’ – either through a large polarised gluon distribution $\Delta g(Q^2)$ in the parton description or due to an anomalous suppression of the slope of the topological susceptibility $\chi'(0)$ in the CPV description. These conjectures are based on assumptions that the appropriate RG invariant quantities, Δq^S or $\hat{\Gamma}_{\Phi_5 pp}$, obey the OZI rule. The motivation for this is particularly strong in the CPV case, where it is supported by a range of evidence from low-energy meson phenomenology in the $U_A(1)$ channel. Moreover, it identifies a fundamental physical mechanism as being at the origin of the ‘proton spin’ suppression – the screening of topological charge by the QCD vacuum.

The two approaches therefore provide related, but complementary, insights into the nature of the ‘proton spin’ effect. Clearly, both insights are needed and both methods have a full part to play in understanding this intriguing and subtle phenomenon.

5. Experiment

In the last year, the SMC collaboration have completed their analysis of the final data from the 1996 run. This is shown in Fig. 6.

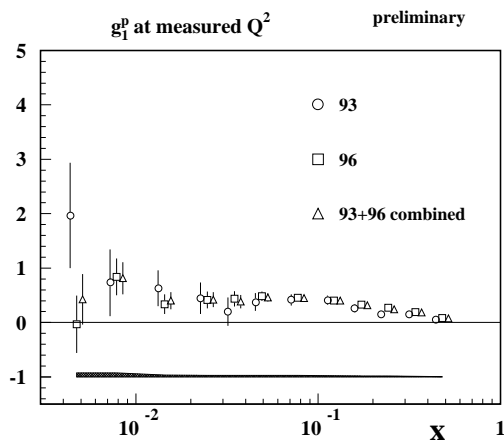


Fig.6 SMC data for g_1^p

Including an uncontroversial extrapolation in the unmeasured region $0.7 < x < 1$, and taking into account the RG scaling from the measured Q^2 for a particular x to the reference value $Q^2 = 10 \text{ GeV}^2$, SMC quote[28] the following result for the first moment of

g_1^p in the measured range $x > 0.003$:

$$\Gamma_1^p(Q^2 = 10\text{GeV}^2)|_{x>0.003} \equiv \int_{0.003}^1 dx g_1^p(x; Q^2) = 0.141 \pm 0.006 \pm 0.008 \pm 0.006 \quad (5.1)$$

where the first error is statistical, the second is systematic and the third is due to the uncertainty in the Q^2 evolution.

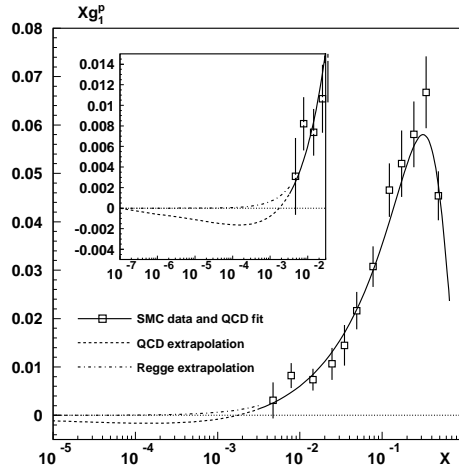


Fig.7 SMC data for xg_1^p including ‘Regge’ and ‘QCD’ small x extrapolations.

The result for the entire first moment depends on how the extrapolation to the unmeasured small x region $x < 0.003$ is performed. See Fig. 7. This is still a controversial issue. Using a simple Regge fit, SMC find $\Gamma_1^p = 0.142 \pm 0.017$ from which they deduce $a^0 = 0.34 \pm 0.17$. Alternatively, using a small x fit in which the parton densities are parametrised at small x at a low Q^2 scale and then extrapolated to higher Q^2 using the perturbative QCD evolution equations[16,29], SMC quote $\Gamma_1^p = 0.130 \pm 0.017$ and $a^0 = 0.22 \pm 0.17$ (all at $Q^2 = 10\text{GeV}^2$). The key feature of the evolution equations is that while $\Delta\Sigma(x, Q^2)$ falls with increasing Q^2 , the polarised gluon distribution $\Delta g(x, Q^2)$ rises. The net effect is that $g_1^p(x, Q^2)$ is driven strongly negative at $Q^2 = 10\text{GeV}^2$ for sufficiently small x . This gives a potentially large negative contribution to the first moment Γ_1^p , but with relatively large errors[29].

Moreover, SMC have recently published an alternative analysis[30] of their data, using a different event selection, this time quoting a slightly lower number for the integral over the measured region of x :

$$\Gamma_1^p(Q^2 = 10\text{GeV}^2)|_{x>0.003} \equiv \int_{0.003}^1 dx g_1^p(x; Q^2) = 0.133 \pm 0.005 \pm 0.006 \pm 0.004 \quad (5.2)$$

Clearly it is premature to draw too strong a conclusion given the large errors on the experimental determinations of Γ_1^p and a^0 and the uncertainty over the small x extrapolation. Future studies of the small x region of g_1^p and the Q^2 scaling behaviour of the gluon distribution $\Delta g(x, Q^2)$ will be important challenges to experimentalists. Nevertheless, it is extremely encouraging that the CPV prediction (4.15) is firmly in the region favoured by the data. This gives us extra confidence that the explanation of the ‘proton spin’ problem in terms of topological charge screening by the QCD vacuum is correct.

6. Semi-Inclusive Polarised DIS

Recently, a new proposal to exploit semi-inclusive DIS in the target fragmentation region to elucidate the ‘proton spin’ effect has been presented[10,11]. The idea is to test the mechanism of topological charge screening, or more precisely the prediction of ‘target independence’, suggested by the CPV method by using semi-inclusive DIS in effect to make measurements of the polarised structure functions of other hadronic targets besides the proton and neutron.

The essence of the target independence conjecture is that for any hadron, the singlet axial charge in eq.(2.3) can be substituted by its OZI value multiplied by a universal (target-independent) suppression factor $s(Q^2)$ determined, up to radiative corrections, by the anomalous suppression of the first moment of the topological susceptibility $\sqrt{\chi'(0)}$. For example, for a hadron containing only u and d quarks, the OZI relation is simply $a^0 = a^8$, so we predict:

$$\Gamma_1 = \frac{1}{12}C_1^{NS} \left(a^3 + \frac{1}{3}(1 + 4s)a^8 \right) \quad (6.1)$$

where

$$s(Q^2) = \frac{C_1^S(\alpha_s)}{C_1^{NS}(\alpha_s)} \frac{a^0(Q^2)}{a^8} \quad (6.2)$$

Since s is target independent, we can use the value measured for the proton to deduce Γ_1 for any other hadron simply from the flavour non-singlet axial charges. From our spectral sum rule estimate of $\sqrt{\chi'(0)}$, we find $s \sim 0.6$ at $Q^2 = 10 \text{ GeV}^2$, while the central values of the results for $a^0(Q^2)$ extracted by SMC from the data give even lower values for s .

The non-singlet axial charges for a hadron \mathcal{B} are given by the matrix elements of the flavour octet axial currents, so can be factorised into products of $SU(3)$ Clebsch-Gordon coefficients and reduced matrix elements. Together with the target independence conjecture, this allows predictions to be made for ratios of the first moments of the polarised structure functions $g_1^{\mathcal{B}}$ for different \mathcal{B} , which involve only group theoretic numbers and the universal suppression factor s . Some of the most interesting are:

$$\Gamma_1^p/\Gamma_1^n = \frac{2s - 1 - 3(2s + 1)F/D}{2s + 2 - 6sF/D} \quad (6.3)$$

$$\Gamma_1^{\Delta^{++}}/\Gamma_1^{\Delta^-} = \Gamma_1^{\Sigma_c^{++}}/\Gamma_1^{\Sigma_c^0} = \frac{2s + 2}{2s - 1} \quad (6.4)$$

where Σ_c^{++} (Σ_c^0) is the state with valence quarks uuc (ddc). The results for Δ and Σ_c are particularly striking because of the $2s - 1$ denominator factor, which is very small for the range of s favoured by experiment. These examples therefore show spectacular deviations from the valence quark counting (OZI) expectations, which would give the ratio 4. They also turn out to be the ones which allow the most clear-cut experimental interpretation.

The proposal of ref.[10] is that these ratios can be realised in semi-inclusive DIS in a kinematical region where the detected hadron h (a pion or D meson in these examples) carries a large target energy fraction, i.e. z approaching 1, with a small invariant momentum transfer. To understand this, we briefly review some of the theory of semi-inclusive DIS.

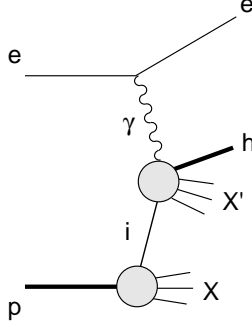


Fig.8 Semi-inclusive DIS: current fragmentation region.

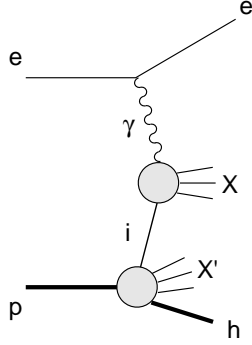


Fig.9 Semi-inclusive DIS: target fragmentation region.

There are two distinct contributions to the semi-inclusive DIS reaction $eN \rightarrow ehX$, coming from the current and target fragmentation regions. These are shown in Figs. 8 and 9. The current fragmentation events are described by parton fragmentation functions $D_i^h(\frac{\tilde{z}}{1-x}, Q^2)$, where i denotes the parton, while the target fragmentation events are described by fracture functions[31] $M_i^{hN}(x, \tilde{z}, Q^2)$ representing the joint probability distribution for producing a parton with momentum fraction x and a detected hadron h (with momentum p'_2) carrying energy fraction \tilde{z} from a nucleon N . The lowest order cross section for polarised semi-inclusive DIS is:

$$x \frac{d\Delta\sigma}{dx dy d\tilde{z}} = \frac{Y_P}{2} \frac{4\pi\alpha^2}{s} \sum_i e_i^2 \left[\Delta M_i^{hN}(x, \tilde{z}, Q^2) + \frac{1}{1-x} \Delta q_i(x, Q^2) D_i^h\left(\frac{\tilde{z}}{1-x}, Q^2\right) \right] \quad (6.5)$$

where $\tilde{z} = E_h/E_N$ (in the photon-nucleon CM frame). The notation is slightly different from section 3. Here, $\Delta q_i(x)$ refers to quarks and antiquarks separately and a sum over both is implied. $\Delta M_i^{hN}(x, \tilde{z}, Q^2)$ is the polarisation asymmetry of the fracture function. The NLO corrections to eq.(6.5) are given in ref.[32].

In fact, for our purposes it is better to use the extended fracture functions introduced recently in refs.[33]. These new fracture functions $\Delta M_i^{hN}(x, z, t, Q^2)$ have an explicit dependence on the invariant momentum transfer t . The original fracture functions are found by integrating over t in the range $t < O(Q^2)$. One of the advantages of the extended fracture functions is that they obey a simple, homogeneous, RG evolution equation:

$$\frac{\partial}{\partial \ln Q^2} \Delta M_i^{hN}(x, z, t, Q^2) = \frac{\alpha_s}{2\pi} \int_x^{1-z} \frac{d\omega}{\omega} \Delta P_{ij}\left(\frac{x}{\omega}, \alpha_s\right) \Delta M_j^{hN}(\omega, x, t, Q^2) \quad (6.6)$$

The differential cross section in the target fragmentation can then be written, analogously to eq.(2.1), as

$$x \frac{d\Delta\sigma^{target}}{dx dy dz dt} = \frac{Y_P}{2} \frac{4\pi\alpha^2}{s} \Delta M_1^{hN}(x, z, t, Q^2) \quad (6.7)$$

where ΔM_1^{hN} is the fracture function equivalent of the inclusive structure function g_1^N , (c.f. eq.(3.2)):

$$\Delta M_1^{hN}(x, z, t, Q^2) = \frac{1}{2} \sum_i e_i^2 \Delta M_i^{hN}(x, z, t, Q^2) \quad (6.8)$$

For z approaching 1, i.e. the hadron carrying a large target energy fraction, this target fragmentation process may be simply modelled by a single Reggeon exchange (see Fig. 10). This corresponds to the approximation

$$\Delta M_1^{hN}(x, z, t, Q^2) \underset{z \sim 1}{\simeq} F(t)(1-z)^{-2\alpha_{\mathcal{B}}(t)} g_1^{\mathcal{B}}(x_{\mathcal{B}}, t, Q^2) \quad (6.9)$$

The notation here is $z = p'_2 \cdot q / p_2 \cdot q$, $x_{\mathcal{B}} = Q^2 / 2k \cdot q$, $1-z = x/x_{\mathcal{B}}$, and $t = -k^2 \ll O(Q^2)$ so that $z \simeq \tilde{z}$. The Reggeon emission factor $F(t)(1-z)^{-2\alpha_{\mathcal{B}}(t)}$ cancels in the ratios of cross sections we consider.

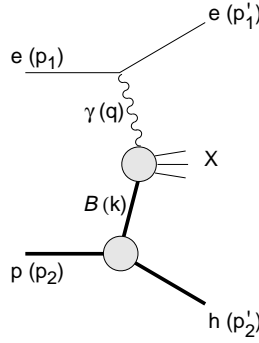


Fig.10 Single Reggeon exchange model of $ep \rightarrow ehX$.

Although single Reggeon exchange is only an approximation to the more fundamental QCD description in terms of fracture functions, it shows particularly clearly how observing semi-inclusive processes at large z with particular choices of h and N amounts in effect to performing inclusive DIS on virtual hadronic targets \mathcal{B} . Since the predictions (6.3,6.4) depend only on the $SU(3)$ properties of \mathcal{B} , together with target independence, they will hold equally well when \mathcal{B} is interpreted as a Reggeon rather than a pure hadron state. For example, from the quark diagram in Fig. 11, we easily see that the semi-inclusive reaction $ep \rightarrow e\pi^- X$ measures $g_1^{\mathcal{B}}$ for $\mathcal{B} = \Delta^{++}$.

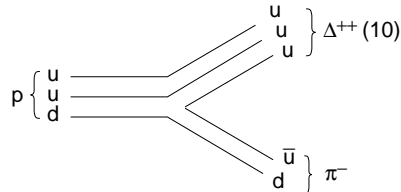


Fig.11 Quark diagram for the $Nh\mathcal{B}$ vertex in the reaction $ep \rightarrow e\pi^- X$ where \mathcal{B} has the quantum numbers of Δ^{++} .

We can therefore make simple predictions for the ratios \mathcal{R} of the first moments of the polarised fracture functions $\int_0^{1-z} dx \Delta M_1^{hN}(x, z, t, Q^2) \simeq \int_0^1 dx_{\mathcal{B}} g_1^{\mathcal{B}}(x_{\mathcal{B}}, t, Q^2)$ for various reactions. We emphasise again that these do not depend on any detailed model of the fracture functions, such as single or even multi-Reggeon exchange. (A more formal justification in terms of the fracture function – cut vertex equivalence[33] is currently under study.) The ratios (6.3,6.4) are obtained in the limit as z approaches 1, where the reaction $eN \rightarrow ehX$ is dominated by the process in which most of the target energy is carried through into the final state h by a single quark. We therefore predict

$$\mathcal{R}\left(\frac{ep \rightarrow e\pi^- X}{en \rightarrow e\pi^+ X}\right) \underset{z \sim 1}{\simeq} \frac{2s+2}{2s-1} \quad (6.10)$$

Similarly for charmed mesons:

$$\mathcal{R}\left(\frac{ep \rightarrow eD^- X}{en \rightarrow eD^0 X}\right) \underset{z \sim 1}{\simeq} \frac{2s+2}{2s-1} \quad (6.11)$$

For strange mesons, on the other hand, the ratio depends on whether the exchanged object has $SU(3)$ quantum numbers in the **8** or **10** representation, so the prediction is less conclusive, e.g.

$$\mathcal{R}\left(\frac{ep \rightarrow eK^0 X}{en \rightarrow eK^+ X}\right) \underset{z \sim 1}{\simeq} \frac{2s-1-3(2s+1)F^*/D^*}{2s-1-3(2s-1)F^*/D^*} \quad (8)$$

$$\frac{2s+1}{2s-1} \quad (10) \quad (6.12)$$

At the opposite extreme, for z approaching 0, the detected hadron carries only a small fraction of the target nucleon energy. In this limit, the ratio of cross section moments for $ep \rightarrow e\pi^-(D^-)X$ and $en \rightarrow e\pi^+(D^0)X$ is simply the ratio of the structure function moments for the proton and neutron.

Interpolating between these limits, we expect the ratio \mathcal{R} in the range $0 < z < 1$ for the reactions $en \rightarrow e\pi^+(D^0)X$ over $ep \rightarrow e\pi^-(D^-)X$ to look like the sketch in Fig. 12.

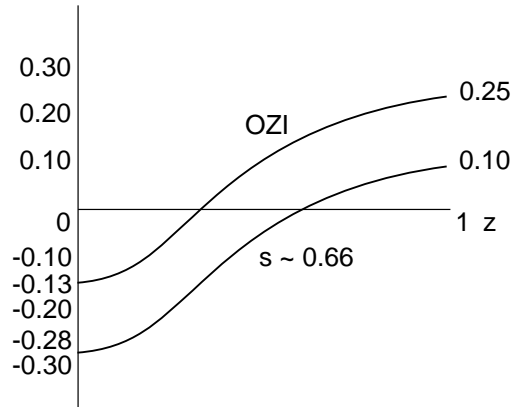


Fig.12 Cross section ratios \mathcal{R} for $en \rightarrow e\pi^+(D^0)X$ over $ep \rightarrow e\pi^-(D^-)X$ between $z \rightarrow 0$ and $z \rightarrow 1$, contrasting the OZI and CPV predictions

The difference between the OZI (or valence quark model) expectations and these predictions based on our target-independent interpretation of the ‘proton spin’ data is therefore quite dramatic, and should give a clear experimental signal.

Since the proposed experiments require particle identification in the target fragmentation region, they are difficult to do at a polarised fixed-target experiments such as COMPASS, or even HERMES, which are better suited to studying semi-inclusive processes in the current fragmentation region. A better option would be a polarised ep collider, such as HERA[34]. To conclude, we shall make some brief comments about the experimental requirements necessary for these predictions to be tested[11].

The first requirement is to measure particles at extremely small angles ($\theta \leq 1$ mrad), corresponding to t less than around 1 GeV^2 . This has already been achieved at HERA in measurements of diffractive and leading proton/neutron scattering. The technique for measuring charged particles involves placing detectors commonly known (but see the discussion session) as ‘Roman Pots’ inside the beam pipe itself. In the present experiments, this detection system is known as the Leading Proton Spectrometer (LPS).

The next point is to notice that the considerations above apply equally to ρ as to π production, since the ratios \mathcal{R} are determined by flavour quantum numbers alone. The particle identification (ID) requirements will therefore be less stringent, especially as the production of leading strange mesons from protons or neutrons is strongly suppressed. However, we require the forward detectors to have good acceptance for both positive and negatively charged mesons $M = \pi, \rho$ in order to measure the ratio (6.10).

The reactions with a neutron target can be measured if the polarised proton beam is replaced by polarised ${}^3\text{He}$. In this case, if we assume that ${}^3\text{He} = Ap + Bn$, the cross section for the production of positive hadrons h^+ measured in the LPS is given by

$$\sigma({}^3\text{He} \rightarrow h^+) \simeq A\sigma(p \rightarrow h^+) + B\sigma(n \rightarrow p) + B\sigma(n \rightarrow M^+) \quad (6.13)$$

The first contribution can be obtained from measurements with the proton beam. However, to subtract the second one, the detectors must have sufficient particle ID at least to distinguish protons from positively charged mesons.

Finally, estimates of the total rates suggest that around 1% of the total DIS events will contain a leading meson in the target fragmentation region where the LPS has non-vanishing acceptance ($z > 0.6$) and in the dominant domain $x < 0.1$. The relevant cross sections are therefore sufficient to allow the ratios \mathcal{R} to be measured.

We conclude that while these proposals undoubtedly pose a challenge to experimentalists, they are nevertheless possible. Given the theoretical importance of the ‘proton spin’ problem and the topological charge screening mechanism, there is therefore strong motivation to perform target fragmentation experiments at polarised HERA.

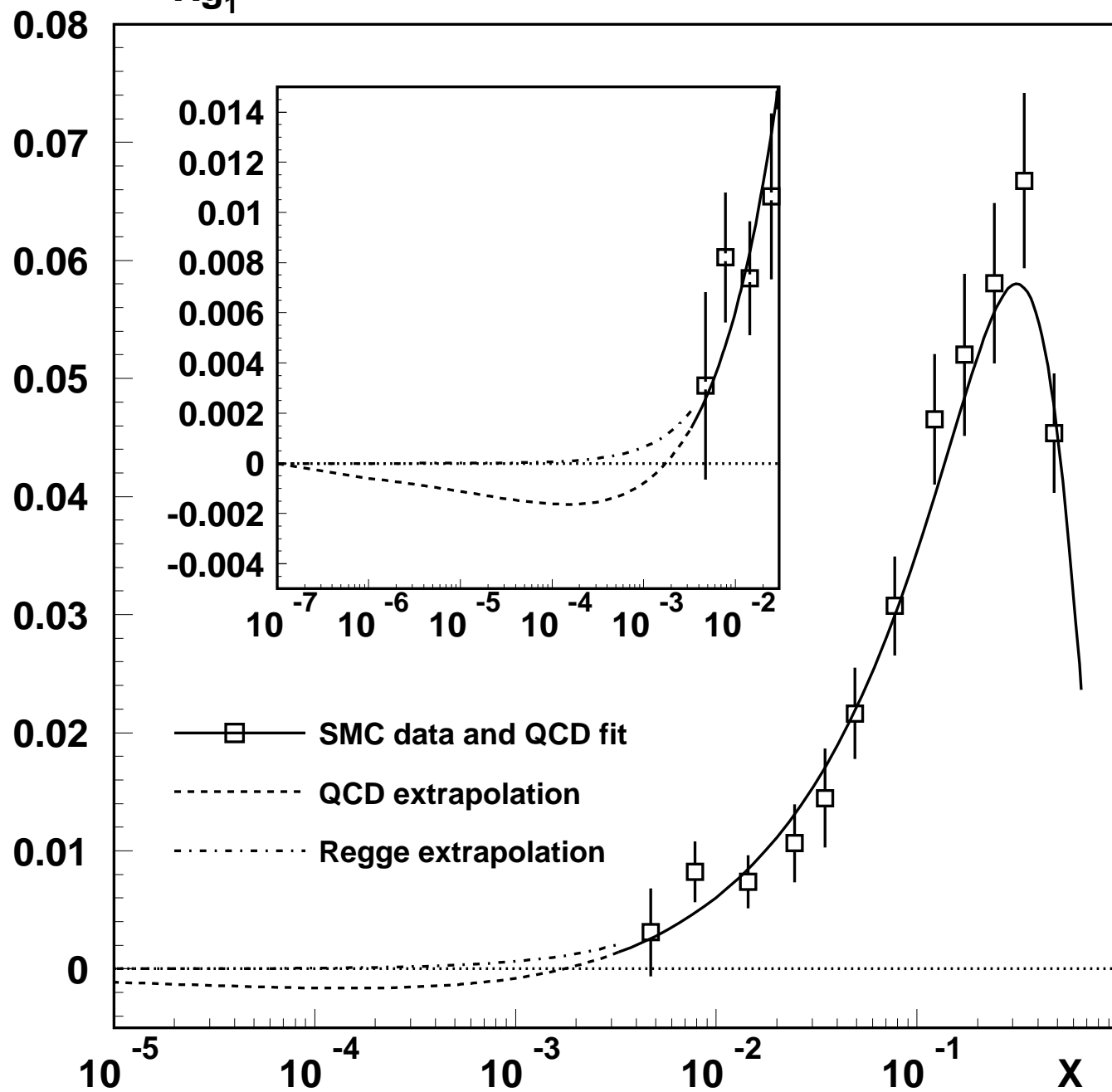
Acknowledgements

I would like to thank the directors of the school, Profs. A. Zichichi, G. ’t Hooft and G. Veneziano for the invitation to lecture in such a wonderful location and the students for their interest and enthusiasm. I am also grateful to D. De Florian, S. Narison and G. Veneziano for their collaboration on the original work presented here. This was supported in part by the EC TMR Network Grant FMRX-CT96-0008 and by PPARC.

References

- [1] EMC Collaboration, J. Ashman *et al.*, *Phys. Lett.* B206 (1988) 364;
Nucl. Phys. B328 (1989) 1.
- [2] J. Ellis and R.L. Jaffe, *Phys. Rev.* D9 (1974) 1444.
- [3] G. Altarelli and G.G. Ross, *Phys. Lett.* B212 (1988) 391.
- [4] G.M. Shore and G. Veneziano, *Phys. Lett.* B244 (1990) 75.
- [5] G.M. Shore and G. Veneziano, *Nucl. Phys.* B381 (1992) 23.
- [6] S. Narison, G.M. Shore and G. Veneziano, *Nucl. Phys.* B433 (1995) 209.
- [7] G. Veneziano, *Mod. Phys. Lett.* A4 (1989) 1605.
- [8] S.L. Adler, *Phys. Rev.* 177 (1969) 2426;
J.S. Bell and R. Jackiw, *Nuovo Cim.* 60 (1969) 47.
- [9] G.M. Shore, *in* Proceedings of the 1998 Zuoz Summer School
on Hidden Symmetries and Higgs Phenomena, hep-ph/9812xxx.
- [10] G.M. Shore and G. Veneziano, *Nucl. Phys.* B516 (1998) 333.
- [11] D. De Florian, G.M. Shore and G. Veneziano, *in* Proceedings of 1997 Workshop
Physics with Polarised Protons at HERA, hep-ph/9711358.
- [12] D. Espriu and R. Tarrach, *Z. Phys* C16 (1982) 77.
- [13] S. Narison, G.M. Shore and G. Veneziano, hep-ph/9812333.
- [14] G. Veneziano, *in* ‘*From Symmetries to Strings: Forty Years of Rochester Conferences*’,
ed. A. Das, World Scientific, 1990.
- [15] X. Ji, *Phys. Rev. Lett.* 78 (1997) 610.
- [16] R.D. Ball, S. Forte and G. Ridolfi, *Phys. Lett.* B378 (1996) 255.
- [17] R.D. Ball, *in* Proceedings, Ettore Majorana International School of Nucleon Structure,
Erice, 1995; hep-ph/9511330.
- [18] R. Ball *et al.*, hep-ph/9609515.
- [19] G.M. Shore and G. Veneziano, *Nucl. Phys.* B381 (1992) 3.
- [20] E. Witten, *Nucl. Phys.* B156 (1979) 269.
- [21] G. Veneziano, *Nucl. Phys.* B159 (1979) 213.
- [22] V.A. Novikov *et al*, *Nucl. Phys.* B237 (1984) 525.
- [23] B.L. Ioffe, *in* Proceedings, Ettore Majorana International School of Nucleon Structure,
Erice, 1995; hep-ph/9511401.
- [24] B.L. Ioffe, Lecture at St. Petersburg Winter School, hep-ph/9804328.
- [25] B.L. Ioffe and A.Yu. Khodzhamiryan, *Yad. Fiz.* 55 (1992) 3045.
- [26] G. Boyd, B. Allés, M. D’Elia and A. Di Giacomo, *in* Proceedings, HEP 97 Jerusalem,
hep-lat/9711025.
- [27] E.V. Shuryak and J.J.M. Verbaarschot, *Phys. Rev.* D52 (1995) 295.
- [28] SMC collaboration, *Phys. Lett.* B412 (1997) 414.
- [29] G. Altarelli, R.D. Ball, S. Forte and G. Ridolfi, *Nucl. Phys.* B496 (1997) 337.
- [30] SMC collaboration, *Phys. Rev.* D58 (1998) 112001.
- [31] L. Trentadue and G. Veneziano, *Phys. Lett.* B323 (1994) 201.
- [32] D. de Florian *et al.*, *Phys. Lett.* B389 (1996) 358.
- [33] M. Grazzini, L. Trentadue and G. Veneziano, *Nucl. Phys.* B519 (1998) 394.
- [34] A. De Roeck and T. Gehrman (eds.), Proceedings of 1997 Workshop,
Physics with Polarized Protons at HERA, hep-ph/9711358.

Xg_1^p



g_1^p at measured Q^2

preliminary

